Published OnlineFirst March 9, 2010; DOI: 10.1158/0008-5472.CAN-09-2821

Integrated Systems and Technologies

Cancer Research

Combined Delivery and Magnetic Resonance Imaging of Neural Cell Adhesion Molecule–Targeted Doxorubicin-Containing Liposomes in Experimentally Induced Kaposi's Sarcoma

Cristina Grange[1], Simonetta Geninatti-Crich[2], Giovanna Esposito[2], Diego Alberti[2], Lorenzo Tei[3], Benedetta Bussolati[1], Silvio Aime[2], and Giovanni Camussi[1]

Abstract

Specific targeting of tumors by combined delivery of drugs and of imaging agents represents an attractive strategy for treatment of cancer. The aim of the present study was to investigate whether neural cell adhesion molecule (NCAM)–targeted liposomes may enhance drug delivery and allow magnetic resonance imaging (MRI) in a severe combined immunodeficient mouse model of NCAM-positive Kaposi's sarcoma. NCAM-binding peptide–coated liposomes loaded with both doxorubicin and a lipophilic gadolinium (Gd) derivative were generated. NCAM-targeted liposomes induced an enhanced *in vitro* doxorubicin internalization within Kaposi's cells as detected by MRI with respect to untargeted polyethylene glycol liposomes. Internalization resulted in enhanced apoptosis. *In vivo* weekly administration of NCAM-targeted liposomes containing 5 mg/kg doxorubicin for 4 consecutive weeks induced a significant reduction of tumor mass and vascularization and enhanced cell necrosis and apoptosis with respect to untargeted liposomes. These effects were associated with an enhanced concentration of doxorubicin within the tumor and a reduced systemic toxicity of doxorubicin. By electron microscopy, NCAM-targeted liposomes were detected mainly within tumor cells whereas the untargeted liposomes were mainly accumulated in the extracellular space. Gd-labeled liposomes allowed the MRI visualization of drug delivery in the tumor region. The intensity of MRI signal was partially hampered by the "quenching" of the attainable relaxation enhancement on endosomal entrapment of the Gd-labeled liposomes. In conclusion, targeting NCAM may be a suitable strategy for specific drug delivery and imaging by liposomes in NCAM-expressing tumors. Moreover, treatment with NCAM-targeted liposomes showed enhanced therapeutic effect and reduced toxicity with respect to untargeted liposomes. *Cancer Res; 70(6); 2180–90. ©2010 AACR.*

Introduction

Targeting tumors or tumor endothelial cells (TEC) with systems that combine delivery of drugs and imaging agents represents one of the most important challenges for the treatment of cancer. Lipid-based nanosized particles have been proved to be suitable as carrier for the delivery of several therapeutic agents (1–3). Due to its superb spatial resolution, magnetic resonance imaging (MRI) seems to be the technique of choice for monitoring drug delivery process and therapeutic output (4). Liposomes seem to be good candidates for carrying both therapeutic and contrast agents, as the payload can be encapsulated in their internal aqueous cavity and/or intercalated in the phospholipid bilayer, thus allowing the transport of both hydrophilic and hydrophobic compounds (5, 6). Clinical applications of liposomes in the delivery of anticancer agents for the treatment of different solid tumors are well established. A specific class of liposomes, named "long time circulating" polyethylene glycol (PEG)–coated liposomes, are able to accumulate in solid tumors as a consequence of increased microvascular permeability and defective lymphatic drainage (7, 8). The extent of passive extravasations is directly dependent on the prolonged residence time of liposomes in the blood stream (9, 10). The most common and widely used chemotherapeutic agent encapsulated in liposomes is doxorubicin (11, 12). The efficacy of doxorubicin incorporated in PEG-coated liposome is under investigation in several tumor models and human clinical trials, such as ovarian, breast, brain, and

Authors' Affiliations: [1]Department of Internal Medicine and [2]Center for Molecular Imaging, Department of Chemistry IFM, University of Turin, Turin, Italy and [3]Department of Environmental and Life Science, University of Piemonte Orientale "A. Avogadro," Alessandria, Italy

Note: Supplementary data for this article are available at Cancer Research Online (http://cancerres.aacrjournals.org/).

C. Grange and S. Geninatti-Crich contributed equally to this work.

Corresponding Author: Giovanni Camussi, Dipartimento di Medicina Interna, Ospedale Maggiore S. Giovanni Battista, Corso Dogliotti 14, 10126 Turin, Italy. Phone: 39-11-6336708; Fax: 39-11-6631184; E-mail: giovanni.camussi@unito.it.

doi: 10.1158/0008-5472.CAN-09-2821

Published OnlineFirst March 9, 2010; DOI: 10.1158/0008-5472.CAN-09-2821

hepatocellular tumors (13–16). Moreover, doxorubicin-containing liposomes are currently used for treatment of some solid tumors, such as Kaposi's sarcoma (17, 18).

The targeting of liposomes to tumor cells is a promising strategy to reduce side effects and improve drug delivery to tumors. To this purpose, liposomes have been functionalized with specific ligands (peptides, monoclonal antibodies, and small organic molecules) able to bind and to internalize receptors expressed on tumor vasculature or on tumor cells (19–24).

We recently reported the expression of the embryonic form of neural cell adhesion molecule (NCAM) by Kaposi's cells and TECs (25). NCAM is an adhesion molecule structurally belonging to the immunoglobulin superfamily that mediates cell-to-cell interactions (26, 27). Moreover, NCAM is expressed by several solid tumors and some leukemias (28). By exploiting a high-affinity NCAM-binding peptide (C3d; refs. 29, 30), we showed the possibility to target NCAM *in vivo* in neo-formed vessels (31).

The aim of this work was to investigate the possibility to use C3d-coated liposomes to enhance drug delivery and allow MRI visualization in an *in vivo* model of Kaposi's sarcoma expressing NCAM. For this purpose, we generated C3d-coated PEG liposomes (C3d lipo) loaded with both doxorubicin and a lipophilic gadolinium (Gd)–DOTA-monamide (DOTAMA) derivative. *In vitro*, we tested the incorporation of C3d lipo within Kaposi's cells and TECs by MRI, the delivery of doxorubicin, and its apoptotic effect. *In vivo*, we evaluated the therapeutic effect of C3d lipo in a model of human Kaposi's sarcoma in severe combined immunodeficient (SCID) mice and the concomitant drug delivery and MRI. The effect of C3d lipo was compared with that of C3d-uncoated PEG liposomes (PEG lipo) containing the same dose of doxorubicin and Gd-DOTAMA derivative.

Materials and Methods

Preparation of doxorubicin-loaded liposomes. POPC (1-palmitoyl-2-oleoyl-*sn*-glycero-3-phosphocholine), DSPE-PEG-PDP {1,2-distearoyl-*sn*-glycero-3-phosphoethanolamine-*N*-poly(ethyleneglycol)-2000-*N*-[3-(2-(pyridyldithio) propionate] ammonium salt}, and DSPE-PEG {1,2-distearoyl-*sn*-glycero-3-phosphoethanolamine-*N*-[methoxy(polyethylene glycol)-2000] ammonium salt} were purchased from Avanti Polar Lipids. Cholesterol and all other chemicals were purchased from Sigma-Aldrich. The lipophilic Gd-DOTAMA $(C18)_2$ was synthesized according to a previously reported procedure (32). Liposomes were prepared by following the thin lipid film hydration method (33). Doxorubicin (hydrochloric salt) incorporation in the internal liposome aqueous phase was done by incubating 0.03 mg of drug per 1 mg of phospholipids for 1 h at 55°C as described (34). The NCAM mimetic C3d peptide (C3 peptide: ASKKPKRNIKA) and the control peptide C3d-Ala, in which Lys^6 and Arg^7 residues are substituted with alanines, were synthesized as previously described (25). For conjugation to thiol-containing molecules, a cysteine residue was added at the COOH terminus of the tetrameric peptides before the lysine backbone (C3d-Cys and C3d-Ala-Cys). A scramble tetrameric peptide (S3d) containing the COOH-terminal cysteine (S3d-Cys-S3d peptide: KAKSRINKAKP) was also synthesized as described in Supplementary Data. The conjugation of the peptides to the liposome was done as described (ref. 35; Supplementary Data). The amount of Gd-DOTAMA$(C18)_2$ incorporated in the liposome was determined by ^1H nuclear magnetic resonance T_1 measurement at 20 MHz, 25°C (Stelar Spinmaster) of the mineralized complex solution (in 6 mol/L HCl at 120°C for 16 h). Doxorubicin encapsulation yield was ~80% and was measured after the peptide conjugation. The hydrated mean diameter of liposomes and the ζ potential were determined using a Malvern dynamic light scattering spectrophotometer (Malvern Zetasizer 3000HS). All samples were analyzed at 25°C in filtered (cutoff, 100 nm) HBS buffer (pH 7). The polydispersity index for all the liposomes prepared in this work was smaller than 0.2. The liposomes were stored at 4°C under argon and used within 2 d from the preparation. FITC-labeled liposomes have been prepared by adding to the lipid mixture 0.1% 1,2-dioleoyl-*sn*-glycero-3-phosphoethanolamine-*N*-(carboxyfluorescein) (ammonium salt).

Cell lines. A primary culture of Kaposi's cells was obtained from a cutaneous lesion of a patient bearing renal allograft under immunosuppressive therapy and previously characterized (36). Kaposi's cells were maintained in culture in RPMI with 10% FCS. TECs were obtained from renal clear cell carcinomas as previously described (37); TECs were maintained in culture in EBM complete medium (Cambrex Bioscience) supplemented with 10% FCS.

Uptake experiments and MRI analysis. Cells were incubated with the liposomes at different Gd concentrations for 3 h at 37°C in the complete medium. Cells were then washed, detached with EDTA (1 mmol/L), washed, and transferred into glass capillaries placed in an agar phantom for MRI analysis. MRI was acquired on a Bruker Avance 300 spectrometer (7 T) equipped with a Micro 2.5 microimaging using a standard T_1-weighted multislice multiecho sequence (TR/TE/NEX, 200:3.3:16; FOV, 1.2 cm; one slice = 1 mm; in-plane resolution, 94 × 94 μm). T_1 measurements of cells were done by using a standard saturation recovery sequence.

Labeling of cell lines and liposomes for* in vitro *binding assay. We labeled the cells with carboxyfluorescein diacetate succinimidyl ester (Vybrant CFDA SE Cell Tracer Kit, Molecular Probe) and the liposomes with the PKH26 Red Fluorescent Cell Linker Kit (Sigma) following the manufacturer's instruction. Cells were incubated for 30 min at 37°C with liposomes (C3d, C3d-Ala, or PEG) and, after washing, were fixed in 3.5% paraformaldehyde containing 2% sucrose. Confocal microscopy analysis was done using a Zeiss LSM 5 Pascal model confocal microscope (Carl Zeiss International). Hoechst 33258 dye (Sigma) was added for nuclear staining. Four different liposome preparations were tested.

Apoptosis assay. For *in vitro* experiments, we incubated cells (Kaposi and TEC), cultured in a 24-well plate, for 1 h with three different liposomes (C3d, C3d-Ala, or PEG) and with doxorubicin alone as positive control. For each stimulus, we used increasing doses of doxorubicin (100, 250, and

Published OnlineFirst March 9, 2010; DOI: 10.1158/0008-5472.CAN-09-2821

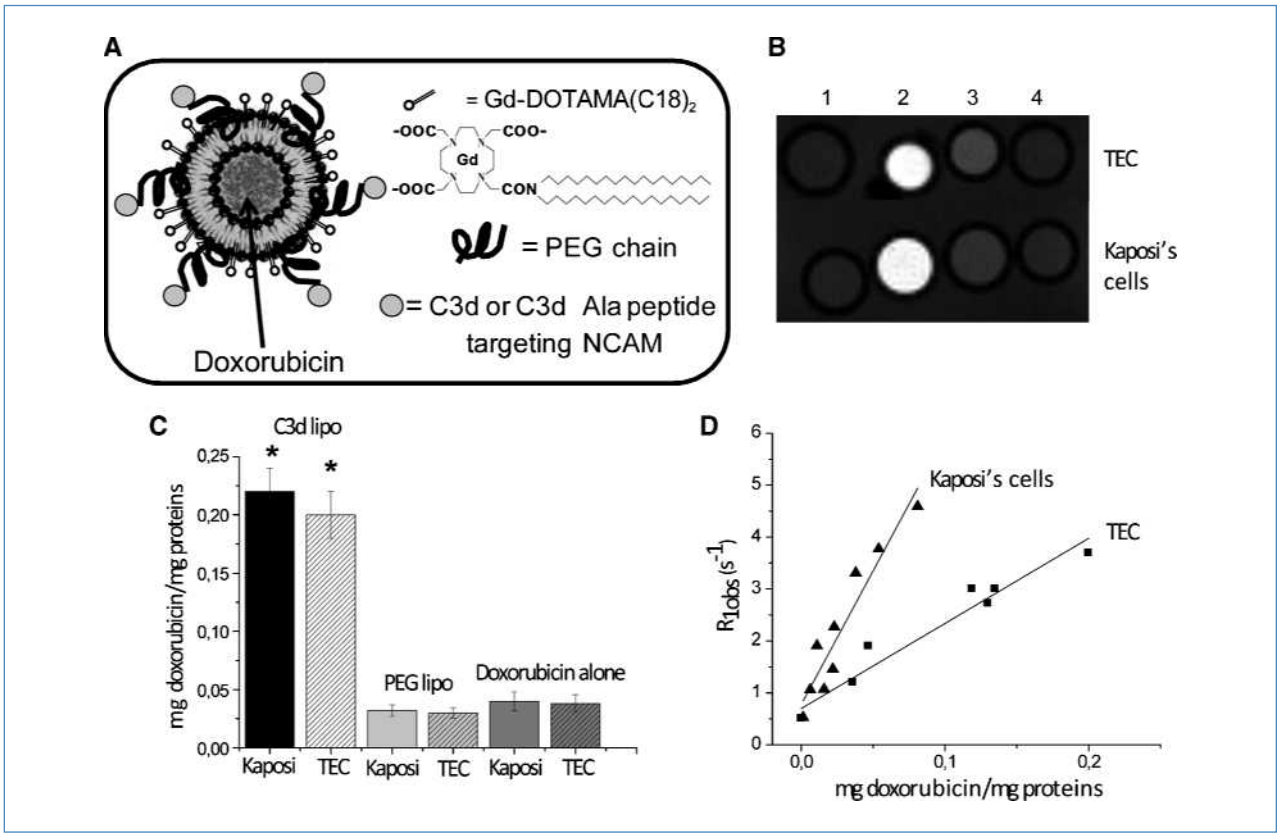

Figure 1. A, schematic representation of liposomes loaded with both doxorubicin and the lipophilic Gd-DOTAMA(C18)$_2$ MRI contrast agent. B, representative T_1-weighted spin echo MRI (measured at 7 T) of an agar phantom containing unlabeled cells (1) or cells incubated with 0.1 mmol/L Gd of C3d lipo (2), C3d-Ala lipo (3), or PEG lipo (4) for 3 h at 37°C. C, doxorubicin intracellular concentration measured in Kaposi's cells and TECs after incubation (for 3 h) with C3d lipo, PEG lipo, and doxorubicin alone, all at 50 μg/mL doxorubicin. Columns, mean of six different experiments; bars, SD. *, $P < 0.01$, C3d lipo versus PEG lipo and doxorubicin alone (ANOVA with Newman-Keuls multicomparison test). D, correlation between observed relaxation rates (R_{1obs} s^{-1}) measured at 7 T and doxorubicin delivered to target cells after 3-h incubation with C3d lipo at increasing concentrations of Gd (0.01–0.1 mmol/L).

500 ng/mL). After 1 h, each sample was washed and medium was replaced with fresh medium. Apoptosis was evaluated after 48 h by terminal deoxynucleotidyl transferase-mediated dUTP nick end labeling (TUNEL) assay (ApopTag Oncor, Millipore). Results are expressed as the mean (± SD) percentage of apoptotic cells per field of four different experiments done in triplicate.

Moreover, we assessed apoptosis by TUNEL assay on slices of tumors recovered at the end of the *in vivo* experiment in SCID mice; paraffin-embedded slices of tumors were deparaffinized, and TUNEL assays were done following the manufacturer's instruction. We counted the number of apoptotic cells per field in 20 randomly chosen sections under ×200 magnification. We expressed the number of apoptotic cells as mean ± SD.

In vivo *therapeutic studies.* All animal experiments were done according to the guidelines for the care and use of research animals and were approved by the local ethics committee. Male mice were 6 to 8 wk of age and their weights were ~22 to 24 g. Kaposi's cells were s.c. implanted in the flank of SCID mice (Charles River Laboratories, Inc.) within growth factor Matrigel (Sigma; day 0); cells (2×10^6) were resuspended in 150 μL of DMEM and added to 150 μL of Matrigel. Ten days after the inoculation of tumor cells, mice were randomly divided into three groups. The first group ($n = 12$) received the functionalized liposomes (C3d lipo), the second group ($n = 12$) was treated with PEG lipo, and the third ($n = 12$), as control, was treated with equal volume of PBS. Each mouse received in the tail vein a dose of liposomes corresponding to 5 mg/kg doxorubicin once per week for 4 consecutive weeks. Mice were monitored two times weekly for body weight and for evidence of tumor or doxorubicin treatment–associated morbidity. Four animals per each group received FITC-labeled liposome in the last i.v. injection for fluorescence staining of liposomes in tumors. Twenty-four hours after the last liposome injection (36 d after the injection of tumor cells) was considered the end of the experiment. Mice were weighed and sacrificed, and the organs (kidney, liver, tumor, brain, and spleen) were recovered for histology. Doxorubicin alone (5 mg/kg) given with the same regimen in six mice or liposomes coated with scramble peptide (see Supplementary Data) were used as controls.

Histologic analysis. For histology, 5-μm-thick paraffin sections of tumor, kidney, liver, brain, and spleen were

Published OnlineFirst March 9, 2010; DOI: 10.1158/0008-5472.CAN-09-2821

routinely stained with H&E (Merck). For the determination of vessel number, sections were stained with Masson trichrome (Masson trichrome Golden, Bio-Optica) and the number of vessels with blood cells inside was counted in 20 randomly chosen sections (×400).

Immunofluorescence. For confocal microscopy analysis, sections from paraffin-embedded tumors treated with FITC liposomes were stained with HLA class I polyclonal antibody (BioLegend). Texas Red goat anti-rabbit IgG (Molecular Probes) was used as secondary antibody. Hoechst 33258 dye (Sigma) was added for nuclear staining.

Electron microscopy. Transmission electron microscopy was done on Karnovsky's fixed, osmium tetraoxide–postfixed tissues and embedded in epoxy resin according to standard procedures (38). Ultrathin sections were stained with uranyl acetate and lead citrate and were examined with a Jeol JEM 1010 electron microscope.

Quantification of doxorubicin in tumor. In eight animals per group, the doxorubicin concentration was measured by spectrofluorimetric analysis as described (ref. 39; see Supplementary Data). Tumors of untreated mice were used as negative control. The results were expressed as mean (± SD) micrograms of doxorubicin per gram of tissue. Fluorescence intensity was measured with a Fluoromax-4 spectrofluorimeter (Horiba Jobin Yvon). Excitation wavelength was positioned at 480 nm and emission wavelength was set at 595 nm. The release of doxorubicin in plasma samples of three healthy individuals and in PBS was evaluated at 5 and 24 h.

Biodistribution and MRI. MRI was acquired at 7 T on a Bruker Advance spectrometer as described above, using a T_1-weighted, fat-suppressed, multislice multiecho protocol (TR/TE/NEX, 250:3.2:6; FOV, 3 cm; one slice = 1 mm). Fat suppression was done by applying a presaturation pulse (90° BW = 1,400 Hz) at the absorption frequency of fat (−1,100 Hz from water). MRI images were acquired 1 d before every administration and 5 and 24 h after treatments. Tumor volumes were estimated from MRI images two times per week. Before MRI examination, animals were anesthetized by injecting tiletamine/zolazepam (Zoletil 100, Virbac, 20 mg/kg) and xylazine (Rompun, Bayer SpA). The mean signal intensity values were calculated in regions of interest drawn on the whole tumors, liver, muscle, spleen, cortical regions of kidneys, and an abdominal vein. Treatment outcome was assessed by calculating the percentage of tumor growth inhibition in the group treated with C3d lipo compared with the group that received PEG lipo or vehicle alone (PBS).

Statistical methods. Data are presented as means ± SD. Differences were determined by Student's t test or ANOVA with the Newman-Keuls multicomparison tests when appropriate. A P value of <0.05 was considered significant.

Results

Preparation and characterization of liposomes. To perform MRI-guided drug delivery, liposomes were loaded with doxorubicin and the Gd-based MRI contrast agent Gd-DOTAMA(C18)$_2$ (Fig. 1A). The millimolar relaxivity (20 MHz, 25°C) of Gd-DOTAMA(C18)$_2$ when incorporated in the liposome formulation was 15.8 $(mmol/L)^{-1}$ s^{-1}. This value is particularly high as a consequence of both the decrease of the molecular mobility after the insertion in the liposome membrane and the relatively fast water exchange rate through the phospholipid bilayer (40). The NCAM targeting liposomes (C3d lipo) were generated using a C3d peptide having a cysteine residue at the COOH terminus conjugated with the PDP functions on the liposome surface. A control liposome (C3d-Ala lipo) functionalized with a nonspecific peptide (C3d-Ala), in which a lysine and an arginine involved in the binding to the receptor of the C3d peptide were replaced by two alanines, was prepared with the same protocol. A liposome functionalized with the C3d scrambled peptide S3d was also prepared as control. The amount of doxorubicin encapsulated in the liposomes remained almost unchanged on conjugation with the peptides. The average liposome hydrodynamic diameters were unaffected on peptide conjugation, and they were 120 ± 20 nm for all investigated formulations as detected by dynamic light scattering measurements. Liposome ζ potentials were −12.5 ± 0.6, +21 ± 2, +9 ± 2, and +18 ± 2 mV for PEG lipo, C3d lipo, C3d-Ala lipo, and S3d lipo, respectively.

As shown in Supplementary Fig. S1, C3d lipo and PEG lipo became stable on incubation at 37°C in PBS and in plasma for 5 and 24 hours. The amount of Gd remained unchanged for PEG and C3d lipo in both media (not shown).

In vitro *liposome cell uptake and MRI.* We previously showed that Kaposi's cells and TECs express on their surface the polysialylated embryonic form of NCAM (25). Liposomes were tested on Kaposi's cells and TECs *in vitro* to evaluate the amount of Gd and doxorubicin taken up by cells and the cytotoxic effect. The results obtained using C3d and C3d-Ala targeted liposomes were compared with those obtained using nontargeted PEG lipo. The MRI acquired at 7 T on Kaposi's cell and TEC pellets (Fig. 1B) showed the specific accumulation of C3d lipo in tumor cells with respect to C3d-Ala lipo and PEG lipo. Figure 1C shows that the intracellular concentration of doxorubicin in Kaposi's cells and TECs incubated with C3d lipo was significantly higher than that found in cells treated with PEG lipo. A good correlation (r = 0.89 and 0.94 for Kaposi's cells and TECs, respectively) between Gd relaxation enhancement and doxorubicin delivered to target cells after the incubation with C3d lipo was found (Fig. 1D). The Gd millimolar relaxivity of internalized C3d lipo was 1.8 $(mmol/L)^{-1}$ s^{-1} at 7 T, a value significantly lower than that measured at the same magnetic field in a 1 mmol/L aqueous solution of C3d lipo [r_{1p} = 4.2 $(mmol/L)^{-1}$ s^{-1}]. This observation supports the view that the liposomes are internalized through receptor-mediated endocytosis. As previously shown (41, 42), the occurrence of a low r_{1p} value is a good indication that the Gd complexes are confined in endosomal vesicles, thus resulting in a "quenching" of the observed relaxivity.

In vitro *apoptotic effect of C3d lipo internalization.* By confocal microscopy, C3d lipo labeled with the red fluorescent dye PKH26 were detected inside Kaposi's cells and TECs after 1 hour of incubation, whereas only minimal internalization was seen using PEG lipo (Fig. 2A). When cells were incubated with liposomes coated with the control C3d-Ala

Published OnlineFirst March 9, 2010; DOI: 10.1158/0008-5472.CAN-09-2821

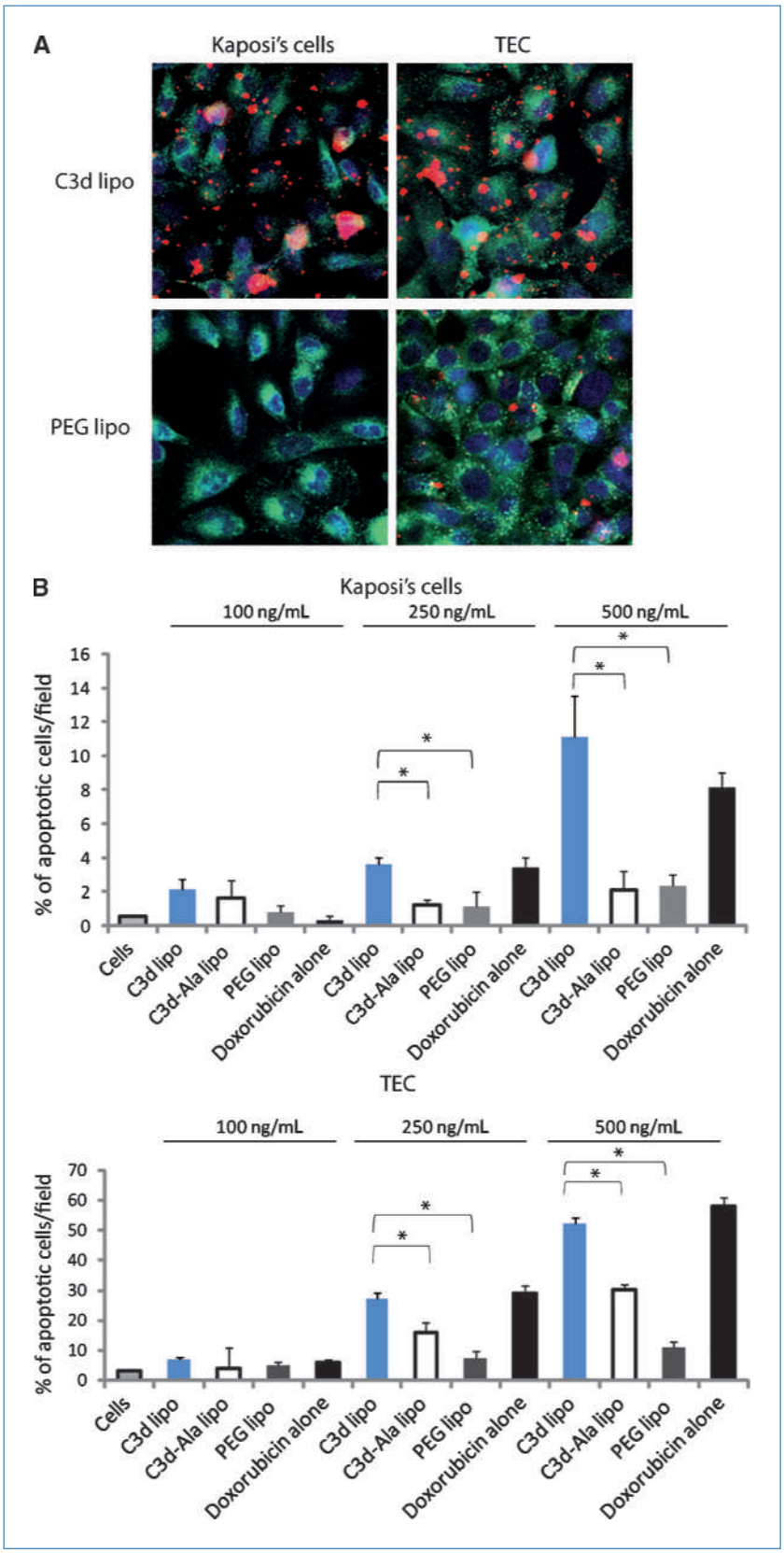

Figure 2. Internalization of liposomes and apoptosis in Kaposi's cells and TECs. A, representative confocal micrographs showing the internalization of C3d lipo after 1 h of incubation at 37°C. Minimal internalization was observed with PEG lipo. Liposomes were labeled with the red dye PKH26, cells with green CSFE, and nuclei with Hoechst 33258 (magnification, ×630). B, apoptosis detected by TUNEL assay. Kaposi's cells and TECs were incubated for 1 h at 37°C with C3d lipo, C3d-Ala lipo, PEG lipo, or doxorubicin alone as described in Materials and Methods. Apoptosis was evaluated after 48 h. Columns, mean of four different experiments performed in triplicate; bars, SD. *, $P < 0.01$, Student's t test.

Published OnlineFirst March 9, 2010; DOI: 10.1158/0008-5472.CAN-09-2821

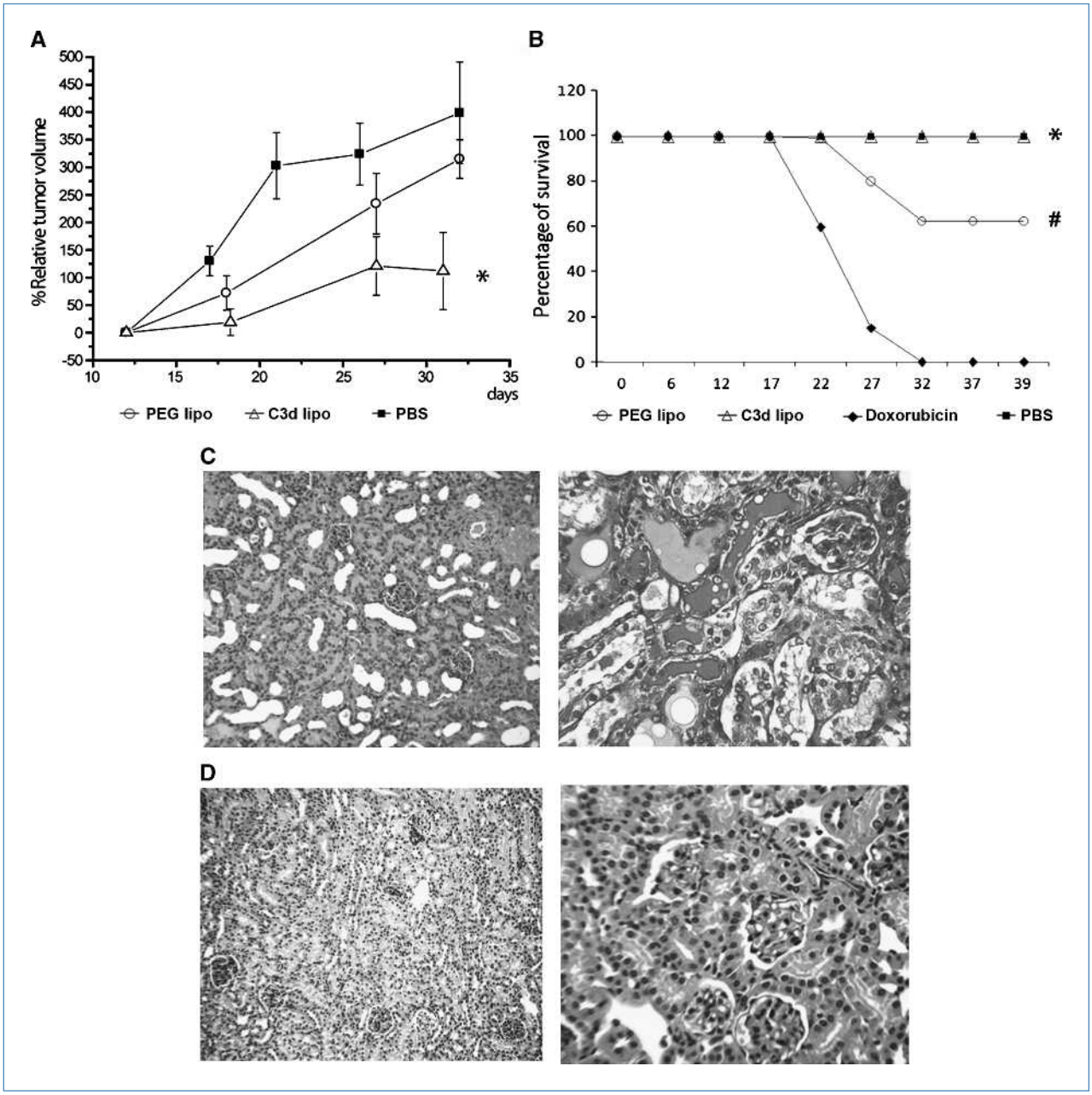

Figure 3. Effect of liposome treatment on SCID mice bearing Kaposi's sarcomas. Ten days after s.c. injection of 2×10^6 tumor cells, mice were treated weekly with 5 mg/kg doxorubicin encapsulated in C3d lipo or in PEG lipo or with vehicle alone (PBS; $n = 12$ per group). A, C3d lipo induced a significant reduction of tumor volume compared with PEG lipo or PBS alone, measured weekly by MRI. *, $P < 0.05$, C3d lipo versus PEG lipo or PBS (ANOVA). B, mortality of mice treated up to day 40 with 5 mg/kg doxorubicin containing C3d lipo, PEG lipo, PBS, or 5 mg/kg doxorubicin alone. *, $P > 0.01$, C3d lipo versus PEG lipo and doxorubicin; #, $P < 0.01$, PEG lipo versus doxorubicin (ANOVA with Newman-Keuls multicomparison test). C, representative micrographs of kidney histology of mice treated with doxorubicin alone showing glomerular injury, tubular casts, necrosis, and atrophy. D, representative micrographs of kidney histology of mice treated with C3d lipo; no significant renal alteration was observed. C and D, left, ×150; right, ×400.

peptide, no internalization was observed (not shown). Apoptosis was evaluated by incubating the cells with different doses of doxorubicin (100, 250, and 500 ng/mL) incorporated within liposomes or used alone as control. A dose-dependent increase in apoptosis was observed. C3d lipo induced a significant higher degree of apoptosis in both Kaposi's cells and TECs compared with apoptosis induced by PEG lipo or C3d-Ala lipo (Fig. 2B).

In vivo *effect of C3d lipo in an experimental model of Kaposi's sarcoma.* SCID mice injected s.c. with 2×10^6 human Kaposi's cells developed a tumor that reached a diameter ranging from 4 to 7 mm after 1 week. Starting from

Published OnlineFirst March 9, 2010; DOI: 10.1158/0008-5472.CAN-09-2821

day 10, mice were treated weekly with 5 mg/kg doxorubicin loaded in C3d lipo or PEG lipo or with vehicle (PBS). As shown in Fig. 3A, the size of tumors detected by MRI of mice treated with C3d lipo was significantly lower than that of mice treated with PEG lipo or PBS. The Kaposi's sarcomas in SCID mice treated with PBS grew subcutaneously without a significant mortality up to day 40 when mice were sacrificed. When treated with doxorubicin alone, all mice died before day 32 as a consequence of doxorubicin toxicity. In these mice, a severe renal injury characterized by tubular necrosis and atrophy, glomerulosclerosis (Fig. 3C), and proteinuria (3,000 ± 500 mg/dL after 15 days) was observed. In contrast, none of the mice treated with C3d lipo and only 30% of those treated with PEG lipo died before the end of the observation period. No significant proteinuria (0–50 mg/dL) or renal histopathologic lesions were observed in mice treated with C3d

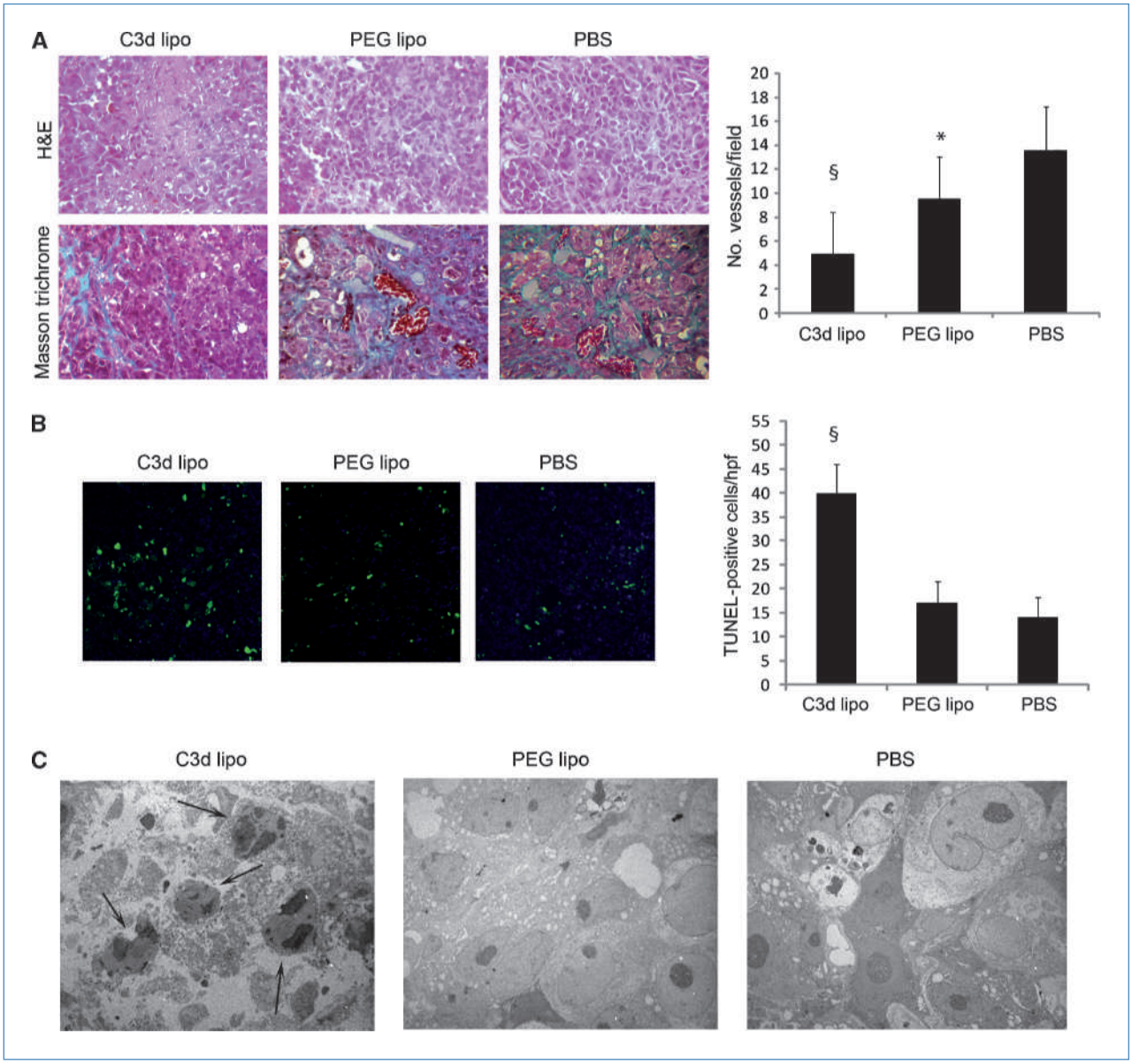

Figure 4. C3d lipo treatment induced apoptosis and necrosis in Kaposi's sarcomas and inhibited vascularization. A, representative micrographs of tumors treated with C3d lipo, PEG lipo, or PBS showing increased cell necrosis and reduced vascularization in C3d lipo with respect to PEG lipo–treated or PBS-treated mice (magnification, ×250). The number of vessels was calculated on trichromic sections as described in Materials and Methods. §, $P < 0.01$, C3d lipo versus PEG lipo and PBS; *, $P < 0.01$, PEG lipo versus PBS (ANOVA with Newman-Keuls multicomparison test). B, representative micrographs and quantitative evaluation of apoptosis detected by TUNEL assay on tumors treated with C3d lipo, PEG lipo, and PBS (magnification, ×200). §, $P < 0.01$, C3d lipo versus PEG lipo and PBS (ANOVA with Newman-Keuls multicomparison test). C, representative micrographs showing transmission electron microscopy of Kaposi's sarcomas developed in SCID mice treated with C3d lipo, PEG lipo, or PBS. Tumors of mice treated with C3d lipo show diffuse necrosis and numerous apoptotic cells (arrows) with characteristic nuclear fragmentation, which are absent or scarce in tumors treated with PEG lipo or PBS (magnification, ×6,000).

Published OnlineFirst March 9, 2010; DOI: 10.1158/0008-5472.CAN-09-2821

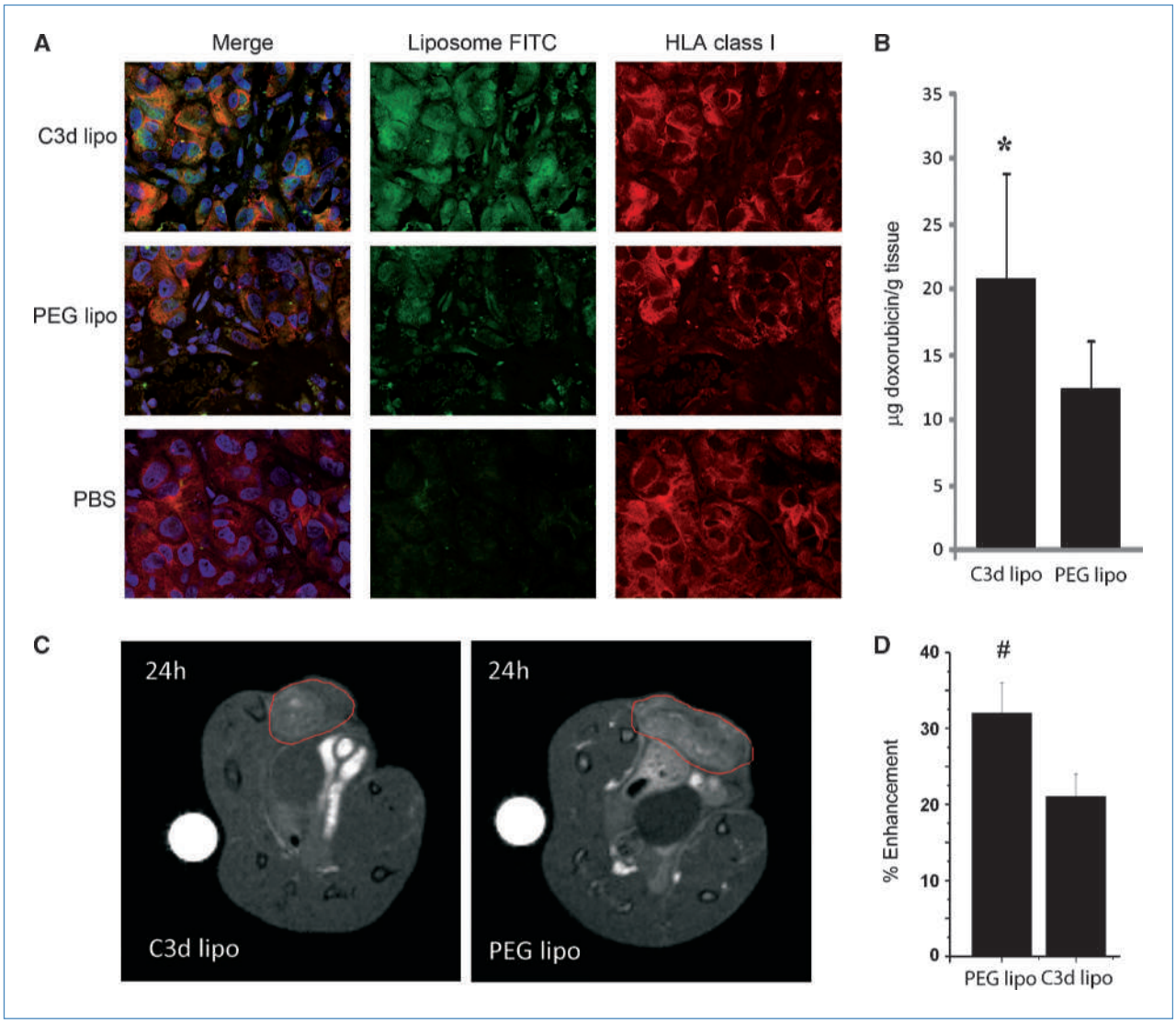

Figure 5. Intratumor accumulation of liposomes, concentration of doxorubicin, and MRI detection. A, representative confocal microscopy of Kaposi's sarcomas treated with C3d lipo, PEG lipo, or PBS analyzed 24 h after the i.v. treatments. Liposomes were labeled with FITC-conjugated lipids (green). The human Kaposi's cells were stained with anti–HLA class I antibodies (red; magnification, ×630). B, extraction and quantification of doxorubicin from tumor tissue ($n = 8$ per group) 24 h after treatment. *, $P < 0.01$ (Student's t test). C, representative T_1-weighted MRI of Kaposi's sarcomas acquired 24 h after the administration of C3d lipo and PEG lipo at a doxorubicin dose of 5 mg/kg corresponding to a Gd dose of 0.023 ± 0.02 mmol/kg. D, percentage of signal intensity enhancement measured in the regions of interest normalized using a standard Gd solution. #, $P < 0.05$ (Student's t test).

lipo. No histologic alteration was observed in the liver, spleen, and brain in all the studied groups.

On histopathologic examinations, Kaposi's sarcomas in mice treated with C3d lipo showed marked areas of necrosis, reduced vascularization (Fig. 4A), and enhanced apoptosis as seen by TUNEL assay and electron microscopy (Fig. 4B and C). The reduction of vessels and the enhanced apoptosis were significantly higher than in mice treated with PEG lipo or PBS. By electron microscopy, tissue dissociation by edema and characteristic fragmentation of apoptotic nuclei were observed in tumors of mice treated with C3d lipo, but not in tumors of mice treated with PEG lipo or PBS (Fig. 4C).

By confocal microscopy, FITC-labeled C3d lipo injected in SCID mice were localized after 24 hours within the human tumor cells, detected as HLA class I–positive cells. In contrast, only very limited incorporation was observed in mice treated with PEG lipo (Fig. 5A). This observation is in agreement with the significantly higher amount of doxorubicin extracted from tumors of mice treated with C3d lipo with respect to those treated with PEG lipo (Fig. 5B).

The accumulation of C3d lipo in tumors was also assessed by MRI. As seen in Fig. 5C, the localization of C3d lipo was clearly detectable within the tumors that showed a reduced size with respect to those treated with PEG lipo. However,

Published OnlineFirst March 9, 2010; DOI: 10.1158/0008-5472.CAN-09-2821

the signal enhancement was lower than that elicited on PEG lipo administration (Fig. 5D). The electron microscopy of tumors showed that PEG lipo were mainly detectable outside of the cells in the interstitial and perivascular areas, whereas the C3d lipo were almost exclusively seen within the cytoplasm of tumor cells (Fig. 6).

Liposome biodistribution, measured by MRI, showed that 5 and 24 hours after injection, the C3d lipo blood content was much lower than that of PEG lipo, with a concomitant increase in liver and spleen uptake (see Supplementary Data). To understand if the different biodistribution and efficacy of PEG and C3d liposomes were due to their different surface charges, a control liposome functionalized with 0.5% of a scrambled peptide of C3d was injected at the same doxorubicin dose (5 mg/kg) in a group of mice. The percentage enhancement measured by MRI (see Supplementary Fig. S2) shows that the amount of scrambled peptide liposome (S3d lipo) accumulated in the tumor is significantly lower than that measured after the injection of C3d lipo.

Discussion

The results of the present study showed that the herein developed liposome functionalized with an anti-NCAM peptide may be used for a combined delivery of a cytotoxic drug and MRI in a model of human Kaposi's sarcoma in SCID mice. Moreover, the targeted liposomes were found to be more efficient for the delivery of drug for the regression of the tumor and less toxic with respect to nontargeted liposomes.

The Kaposi's sarcoma is an angiogenic tumor often associated with conditions of immune system impairment, such as HIV1 infections or posttransplantation immunosuppressive therapy (43–45). We have recently found that Kaposi's cells and tumor-derived endothelial cells express NCAM on their surface. NCAM is a widely expressed molecule during embryogenesis, which is downregulated in the course of differentiation to be reexpressed in some tumors and TECs (25). By exploiting NCAM expression, we recently developed a strategy to detect *in vivo* by MRI the neo-formed vessels using a NCAM peptide (C3d; ref. 31). In the present study, the model of Kaposi's sarcoma implanted in SCID mice was chosen because treatment with liposome containing doxorubicin is currently used as a therapeutic strategy for this tumor (46, 47). Doxorubicin incorporation into liposomes seems to reduce the systemic toxicity of the drug (48).

In the present study, we found that C3d-coated liposomes loaded with both doxorubicin and Gd-DOTAMA(C18)$_2$ were internalized and induced apoptosis of Kaposi's cells and TECs significantly more efficiently than did the uncoated

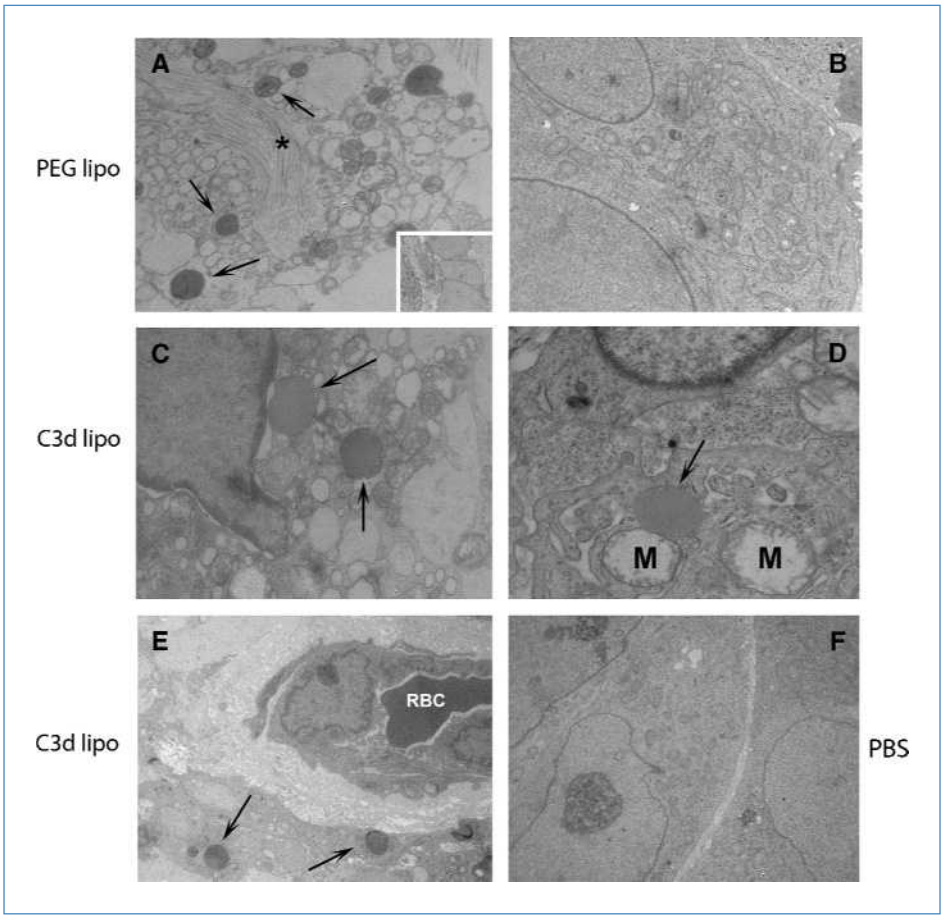

Figure 6. Representative transmission electron microscopy of Kaposi's sarcomas treated with PEG lipo or C3d lipo. A, Gd-labeled PEG lipo are predominantly observed in perivascular interstitial space. Arrows, liposomes; *, extracellular matrix. B, PEG lipo internalization is absent in tumor cells. C and D, representative electron microscopy showing the internalization of C3d lipo within tumor cells, which display alteration in the cytoplasmic organic swelling and disorganization of mitochondria (M). E, liposome internalization in perivascular cells. F, representative micrograph of tumor cells of mice injected with PBS. Original magnifications, ×15,000 (A, B, E, and F) and ×20,000 (C and D).

Published OnlineFirst March 9, 2010; DOI: 10.1158/0008-5472.CAN-09-2821

PEG liposomes. This indicated that the NCAM-C3d interaction allowed a specific internalization of C3d lipo whereas PEG lipo mainly remained extracellular.

The incorporation of doxorubicin in PEG-coated liposomes alters the pharmacokinetics of the drug, resulting in a smaller volume of distribution and slower plasma clearance than free doxorubicin, thus allowing an extravasation at the site of enhanced permeability. In contrast, C3d lipo were rapidly internalized within the Kaposi's sarcoma cells bearing NCAM, with a reduced persistence in plasma. This resulted in a more efficient reduction of tumor mass and vascularization. These effects were related to an enhanced *in vivo* intracellular accumulation of C3d lipo within the tumors associated with an enhanced intratumor concentration of doxorubicin with respect to PEG lipo. Moreover, C3d lipo were found to be less toxic than free doxorubicin and PEG lipo.

The specific delivery of C3d lipo to targeted Kaposi's cells was confirmed by MRI both *in vitro* and *in vivo*. MRI showed the reduced size of tumors in C3d lipo–treated mice and allowed detection of drug delivery within the tumors. However, the intensity of MRI signal enhancement within the tumors was lower than that obtained with PEG liposomes. This is likely due to the internalization of paramagnetic liposomes into cells that can limit the attainable relaxation enhancement as a consequence of the reduced water exchange across the barriers among the different compartments. The efficiency of PEG lipo is more than two times higher than that of C3d lipo because of its prevalent extracellular distribution. In fact, by electron microscopy, PEG lipo were mainly detected outside of the cells in the interstitial and perivascular areas whereas the C3d lipo were almost exclusively seen within the cytoplasm of tumor cells. Furthermore, 24 hours after the injection, a good amount of PEG lipo is still circulating in the blood stream, yielding an extra signal enhancement contribution in the tumor region.

In conclusion, NCAM-targeted liposomes specifically delivered doxorubicin and induced regression of Kaposi's sarcoma in SCID mice, suggesting that targeting NCAM may be a therapeutic strategy for NCAM-positive tumors. Indeed, the therapeutic efficacy and the toxicity of doxorubicin were improved when incorporated in the C3d liposomes. Finally, the use of Gd-labeled liposomes allowed the concomitant MRI visualization of the drug delivery in the tumor region.

Disclosure of Potential Conflicts of Interest

No potential conflicts of interest were disclosed.

Acknowledgments

We thank Dr. Massimo Visigalli (Bracco Imaging, Colleretto Giacosa, Italy) for the synthesis of Gd-DOTAMA(C18)$_2$.

Grant Support

Regione Piemonte Nano-IGT project (Converging Technologies) and Ricerca Scientifica Applicata, Istituto Superiore di Sanità (40F.19), Associazione Italiana per la Ricerca sul Cancro, ENCITE project (FP7-HEALTH-2007-A), DiMI (CT-2005-512146) EU NoEs, and Meditrans (NMP4-CT-2006-026668).

The costs of publication of this article were defrayed in part by the payment of page charges. This article must therefore be hereby marked *advertisement* in accordance with 18 U.S.C. Section 1734 solely to indicate this fact.

Received 07/31/2009; revised 12/18/2009; accepted 01/14/2010; published OnlineFirst 03/09/2010.

References

1. Allen TM. Ligand-targeted therapeutics in anticancer therapy. Nat Rev Cancer 2002;2:750–63.
2. Haley B, Frenkel E. Nanoparticles for drug delivery in cancer treatment. Urol Oncol 2008;26:57–64.
3. Schiffelers RM, Storm G. Liposomal nanomedicines as anticancer therapeutics: beyond targeting tumor cells. Int J Pharm 2008;364:258–64.
4. Li C, Penet MF, Winnard P, Jr., Artemov D, Bhujwalla ZM. Image-guided enzyme/prodrug cancer therapy. Clin Cancer Res 2008;14:515–22.
5. Koning GA, Krijger GC. Targeted multifunctional lipid-based nanocarriers for image-guided drug delivery. Anticancer Agents Med Chem 2007;7:425–40.
6. Schwendener RA. Liposomes in biology and medicine. Adv Exp Med Biol 2007;620:117–28.
7. Maeda H, Wu J, Sawa T, Matsumura Y, Hori K. Tumor vascular permeability and the EPR effect in macromolecular therapeutics: a review. J Control Release 2000;65:271–84.
8. Greish K. Enhanced permeability and retention of macromolecular drugs in solid tumors: a royal gate for targeted anticancer nanomedicines. J Drug Target 2007;15:457–64.
9. Romberg B, Hennink WE, Storm G. Sheddable coatings for long-circulating nanoparticles. Pharm Res 2008;25:55–71.
10. Immordino ML, Dosio F, Cattel L. Stealth liposomes: review of the basic science, rationale, and clinical applications, existing and potential. Int J Nanomedicine 2006;1:297–315.
11. Garde SV, Forté AJ, Ge M, et al. Binding and internalization of NGR-peptide-targeted liposomal doxorubicin (TVT-DOX) in CD13-expressing cells and its antitumor effects. Anticancer Drugs 2007;18:1189–200.
12. Gabizon A, Martin F. Polyethylene glycol-coated (pegylated) liposomal doxorubicin. Rationale for use in solid tumours. Drugs 1997;54:15–21.
13. Main C, Bojke L, Griffin S, et al. Topotecan, pegylated liposomal doxorubicin hydrochloride and paclitaxel for second-line or subsequent treatment of advanced ovarian cancer: a systematic review and economic evaluation. Health Technol Assess 2006;10:1–132.
14. Ulrich-Pur H, Kornek GV, Haider K, et al. Phase II trial of pegylated liposomal doxorubicin (Caelyx) plus gemcitabine in chemotherapeutically pretreated patients with advanced breast cancer. Acta Oncol 2007;46:208–13.
15. Wagner S, Peters O, Fels C, et al. Pegylated-liposomal doxorubicin and oral topotecan in eight children with relapsed high-grade malignant brain tumors. J Neurooncol 2008;86:175–81.
16. Piguet AC, Semela D, Keogh A, et al. Inhibition of mTOR in combination with doxorubicin in an experimental model of hepatocellular carcinoma. J Hepatol 2008;49:78–87.
17. Northfelt DW, Martin FJ, Working P, et al. Doxorubicin encapsulated in liposomes containing surface-bound polyethylene glycol: pharmacokinetics, tumor localization, and safety in patients with AIDS-related Kaposi's sarcoma. J Clin Pharmacol 1996;36:55–63.
18. Allen TM. Long-circulating (sterically stabilized) liposomes for targeted drug delivery. Trends Pharmacol Sci 1994;15:215–20.
19. Villares GJ, Zigler M, Wang H, et al. Targeting melanoma growth and

Published OnlineFirst March 9, 2010; DOI: 10.1158/0008-5472.CAN-09-2821

metastasis with systemic delivery of liposome-incorporated protease-activated receptor-1 small interfering RNA. Cancer Res 2008; 68:9078–86.
20. Gosk S, Moos T, Gottstein C, Bendas G. VCAM-1 directed immunoliposomes selectively target tumor vasculature *in vivo*. Biochim Biophys Acta 2008;1778:854–63.
21. Roth P, Hammer C, Piguet AC, Ledermann M, Dufour JF, Waelti E. Effects on hepatocellular carcinoma of doxorubicin-loaded immunoliposomes designed to target the VEGFR-2. J Drug Target 2007;15: 623–31.
22. Zhao H, Wang JC, Sun QS, Luo CL, Zhang Q. RGD-based strategies for improving antitumor activity of paclitaxel-loaded liposomes in nude mice xenografted with human ovarian cancer. J Drug Target 2009;17:10–8.
23. Anhorn MG, Wagner S, Kreuter J, Langer K, von Briesen H. Specific targeting of HER2 overexpressing breast cancer cells with doxorubicin-loaded trastuzumab-modified human serum albumin nanoparticles. Bioconjug Chem 2008;19:2321–31.
24. Chang DK, Lin CT, Wu CH, Wu HC. A novel peptide enhances therapeutic efficacy of liposomal anti-cancer drugs in mice models of human lung cancer. PLoS ONE 2009;4.
25. Bussolati B, Grange C, Bruno S, et al. Neural-cell adhesion molecule (NCAM) expression by immature and tumor-derived endothelial cells favors cell organization into capillary-like structures. Exp Cell Res 2006;312:913–24.
26. Rønn LCB, Olsen M, Ostergaard S, et al. Identification of a neuritogenic ligand of the neural cell adhesion molecule using a combinatorial library of synthetic peptides. Nat Biotechnol 1999;17:1000–5.
27. Walsh FS, Doherty P. Neural cell adhesion molecules of the immunoglobulin superfamily: role in axon growth and guidance. Annu Rev Cell Dev Biol 1997;13:425–56.
28. Jensen M, Berthold F. Targeting the neural cell adhesion molecule in cancer. Cancer Lett 2007;258:9–21.
29. Rønn LC, Berezin V, Bock E. The neural cell adhesion molecule in synaptic plasticity and ageing. Int J Dev Neurosci 2000;18:193–9.
30. Kiryushko D, Kofoed T, Skladchikova G, Holm A, Berezin V, Bock E. Identification of a neuritogenic ligand of the neural cell adhesion molecule using a combinatorial library of synthetic peptides. J Biol Chem 2003;278:12325–34.
31. Geninatti Crich S, Bussolati B, Tei L, et al. Magnetic resonance visualization of tumor angiogenesis by targeting neural cell adhesion molecules with the highly sensitive gadolinium-loaded apoferritin probe. Cancer Res 2006;66:9196–201.
32. Anelli PL, Lattuada L, Lorusso V, Schneider M, Tournier H, Uggeri F. Mixed micelles containing lipophilic gadolinium complexes as MRA contrast agents. MAGMA 2001;12:114–20.
33. Olson F, Hunt CA, Szoka FC, Vail WJ, Papahadjopoulos D. Preparation of liposomes of defined size distribution by extrusion through polycarbonate membranes. Biochim Biophys Acta 1979;557:9–23.
34. Abraham SA, Waterhouse DN, Mayer LD, Cullis PR, Madden TD, Bally MB. The liposomal formulation of doxorubicin. Methods Enzymol 2005;391:71–97.
35. Hermanson GT. Bioconjugate techniques. Pyridyl disulfides. San Diego (CA): Academic Press; 1996, p. 151.
36. Deregibus MC, Cantaluppi V, Doublier S, et al. HIV-1-Tat protein activates phosphatidylinositol 3-kinase/AKT-dependent survival pathways in Kaposi's sarcoma cells. J Biol Chem 2002;277: 25195–202.
37. Bussolati B, Deambrosis I, Russo S, Deregibus MC, Camussi G. Altered angiogenesis and survival in human tumor-derived endothelial cells. FASEB J 2003;17:1159–61.
38. Camussi G, Kerjaschki D, Gonda M, et al. Expression and modulation of surface antigens in cultured rat glomerular visceral epithelial cells. J Histochem Cytochem 1989;37:1675–87.
39. Goren D, Horowitz AT, Tzemach D, Tarshish M, Zalipsky S, Gabizon A. Nuclear delivery of doxorubicin via folate-targeted liposomes with bypass of multidrug-resistance efflux pump. Clin Cancer Res 2000;6: 1949–57.
40. Fossheim SL, Fahlvik AK, Klaveness J, Muller RN. Paramagnetic liposomes as MRI contrast agents: influence of liposomal physicochemical properties on the *in vitro* relaxivity. Magn Reson Imaging 1999;17:83–89.
41. Terreno E, Geninatti Crich S, Belfiore S, et al. Effect of the intracellular localization of a Gd-based imaging probe on the relaxation enhancement of water protons. Magn Reson Med 2006;55:491–7.
42. Esposito G, Geninatti Crich S, Aime S. Efficient cellular labeling by CD44 receptor-mediated uptake of cationic liposomes functionalized with hyaluronic acid and loaded with MRI contrast agents. ChemMedChem 2008;3:1858–62.
43. Nakamura S, Salahuddin SZ, Biberfeld P, et al. Kaposi's sarcoma cells: long-term culture with growth factor from retrovirus-infected $CD4^+$ T cells. Science 1988;242:426–30.
44. Mitsuyasu RT. Update on the pathogenesis and treatment of Kaposi sarcoma. Curr Opin Oncol 2000;12:174–80.
45. Albini A, Paglieri I, Orengo G, et al. The β-core fragment of human chorionic gonadotrophin inhibits growth of Kaposi's sarcoma-derived cells and a new immortalized Kaposi's sarcoma cell line. AIDS 1997;11:713–21.
46. Sharpe M, Easthope SE, Keating GM, Lamb HM. Polyethylene glycol-liposomal doxorubicin: a review of its use in the management of solid and haematological malignancies and AIDS-related Kaposi's sarcoma. Drugs 2002;62:2089–126.
47. Krown SE, Northfelt DW, Osoba D, Stewart JS. Use of liposomal anthracyclines in Kaposi's sarcoma. Semin Oncol 2004;31:36–52.
48. Vail DM, Amantea MA, Colbern GT, Martin FJ, Hilger RA, Working PK. Pegylated liposomal doxorubicin: proof of principle using preclinical animal models and pharmacokinetic studies. Semin Oncol 2004;31:16–35.

Published OnlineFirst March 9, 2010; DOI: 10.1158/0008-5472.CAN-09-2821

Cancer Research
The Journal of Cancer Research (1916–1930) | The American Journal of Cancer (1931–1940)

AACR American Association for Cancer Research

Combined Delivery and Magnetic Resonance Imaging of Neural Cell Adhesion Molecule–Targeted Doxorubicin-Containing Liposomes in Experimentally Induced Kaposi's Sarcoma

Cristina Grange, Simonetta Geninatti-Crich, Giovanna Esposito, et al.

Cancer Res 2010;70:2180-2190. Published OnlineFirst March 9, 2010.